

All-PP composites (PURE[®]) with unidirectional and cross-ply lay-ups: dynamic mechanical thermal analysis

T. Abraham, K. Banik, J. Karger-Kocsis*

Institute for Composite Materials (Institut für Verbundwerkstoffe GmbH), Technical University Kaiserslautern, D-67663 Kaiserslautern, Germany

Received 19 May 2007; accepted in revised form 3 July 2007

Abstract. All polypropylene (all-PP) composite laminates with unidirectional (UD) and cross-ply (CP) lay-ups were produced by hot consolidation from oriented coextruded PP tapes (PURE[®]). The consolidation of the tapes, wound on a steel plate, occurred in autoclave vacuum bag molding. The set processing conditions resulted in all-PP laminates of high rigidity as the PP copolymer surface layers of the tapes were molten and thus forming the matrix, while their PP homopolymer core remained unaffected and thus fulfilled its role as reinforcement. Specimens cut off from the laminates were subjected to dynamic mechanical thermal analysis (DMTA) in a broad temperature range ($T = -50 \dots 120^\circ\text{C}$) at various frequencies ($f = 10^{-2} \dots 10^1$). For the DMTA results the time-temperature superposition principle was adopted and master curves in the form of storage modulus vs. frequency ($f = 10^{-9} \dots 10^{20}$) and loss factor vs. frequency were created.

Keywords: polymer composites, thermal properties, polypropylene, all-polypropylene composite, PURE[®]

1. Introduction

The original concept of self-reinforced composite, a composite with matrix and reinforcement from the same polymer, was presented by Capiati and Porter [1] three decades ago for high density polyethylene. Later this concept was adopted to polypropylene (PP) [2–5], polyethylene [6–10], polyethylene terephthalate [11–13], polyethylene naphthalate [14], poly(methyl methacrylate) [15–18], polyamide [19] and liquid crystal polymers [20, 21]. Particularly, in a series of recent papers, Alcock and coworkers [22–24] described composite materials in which both the reinforcement and the matrix were based on PP. The related composites under the trade name of PURE[®] are produced from highly oriented co-extruded tapes having a skin-core-skin (A:B:A) morphology. The skin layer (A) contains a PP random copolymer, whereas the core layer (B) is composed of PP homopolymer.

Since the copolymer skin layer has a melting temperature below that of the homopolymer core, self-reinforced (also termed as homocomposites or all-PP composites) PP systems can be produced using a suitable processing window. Note that during consolidation the PP copolymer forms the matrix, while the highly oriented PP homopolymer fraction acts as continuous reinforcement. This approach (i. e. copolymer for the matrix and homopolymer for the reinforcement) can be used to produce all-PP composites using the film stacking technique, as well [25]. The most recent development with all-PP composites is to exploit the polymorphism-related difference in the melting range between the beta- (giving the matrix) and alpha-phases (serving as reinforcement) PPs [26, 27]. All-PP composites are characterized by their outstanding mechanical properties at very low density. Their main advantage over conventional glass fiber reinforced ver-

*Corresponding author, e-mail: karger@ivw.uni-kl.de
© BME-PT and GTE

sions is the easy recycling, because they comprise a single material (PP).

It is well known that the physical properties of a polymeric material are strongly dependent on its morphology, structure and relaxation processes corresponding to internal changes and molecular motions. Dynamic mechanical measurements over a wide temperature or frequency ranges are useful to understand the viscoelastic behavior and provide valuable insights into the relationship between structure, morphology and properties of polymers and related composites. Structure-property relationships in fiber reinforced PP composites were disclosed based on dynamic mechanical thermal analysis (DMTA) data (e.g. [28]). However, DMTA was less considered for all-PP composites [29].

The main aim of this study is to investigate the DMTA response of highly oriented PP tapes and all-PP composite laminates of various lay-up manufactured using these PP tapes. DMTA tests were run at different frequencies over a wide range of temperatures. By using the DMTA data, master curves can be created to predict the performance of all-PP composites at much higher frequencies than achievable in the laboratory.

2. Experimental

2.1. Manufacture of laminates

The tape used for the preparation of the composite laminates was a highly oriented, co-extruded PP tape (PURE[®]) manufactured at Lankhorst-Indutech (Sneek, The Netherlands). Characteristics of PP tapes used for the preparation of the laminates are summarized in Table 1. The manufacture of the PP laminates involved a two-stage process – winding of the PP tapes, both unidirectional (0°)(UD) and cross-ply (0/90°)(CP), and consolidation of the related tape assemblies at a suitable temperature and pressure in an autoclave. The schematic of the

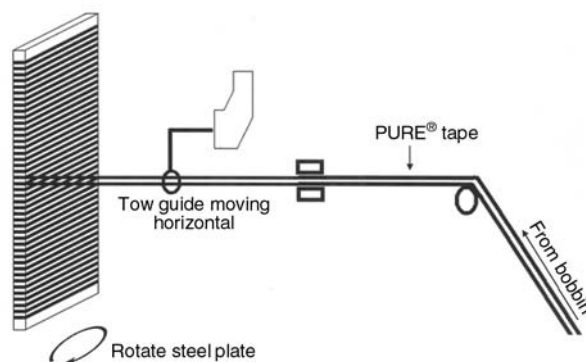


Figure 1. Scheme of the tape winding process for the fabrication of all-PP composites (in this case with UD structure)

tape winding process is shown in Figure 1. Using a typical winding machine, supplied by Bolenz & Schaefer Maschinenfabrik (Biedenkopf, Germany), PP tapes were wound from a bobbin onto a thin steel plate rotating at a constant speed of 40 rpm. In each case, the total number of layers was kept the same (30 layers). For producing CP laminates, the winding direction on the steel plate was sequentially changed. After laying two UD layers, another two layers of tapes were positioned perpendicular to them. A similar process for manufacturing UD all-PP composites from coextruded tapes has already been reported in the literature by Alcock *et al.* [22]. To consolidate the all-PP composites, the steel plate with the wrapped plies was placed in between two other steel plates inside a vacuum bag. This bag was connected to a vacuum pump applying negative pressure inside the bag. The entire bag was then placed inside an autoclave obtained from the Scholz Maschinenbau GmbH, (Coesfeld, Germany) and slowly heated to the consolidation temperature (T_C) of 145°C. A thermocouple was used to monitor the temperature rise in the specimen during heating. Simultaneously, the vacuum pump was started when the pressure began to grow in the autoclave until reaching the consolidation pressure ($P = 24$ bar). The time needed by the specimen to reach the consolidation temperature was considerably longer ($t_3 - t_1 \sim 90$ min) than the air temperature inside the autoclave ($t_2 - t_1$). Once the specimen reached T_C , a constant consolidation time ($t_4 - t_3$) of 30 min was given. After consolidation, the laminates were cooled to the release temperature (T_R) of 30°C. The pressure was released when the air temperature inside the autoclave reached 30°C. Cooling of the laminate ($t_5 - t_4$) took approx-

Table 1. Properties of the PURE[®] PP tape used based on the information of the manufacturer

Width	~2.3 mm
Thickness	~50 μ m
Density, ρ	0.829 g/cm ³
Composition	copolymer:homopolymer: copolymer
Tensile modulus (ISO 527)	15 \pm 2 GPa
Tensile strength (ISO 527)	~500 MPa
Elongation at break (ISO 527)	~6%
Shrinkage at 145°C for 30 min	5.5 \pm 0.5%

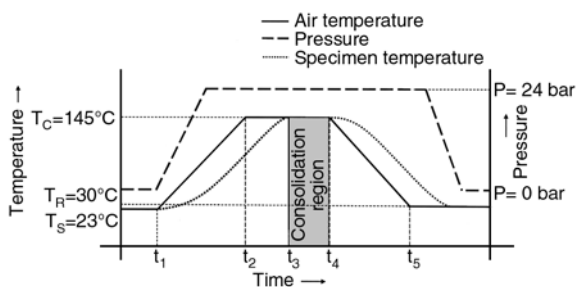


Figure 2. Time-temperature and time-pressure profiles during the autoclave vacuum bag consolidation of the all-PP composites

imately 60 min. Identical consolidation parameters were used for the production of both UD and CP lay-ups. The time-temperature and time-pressure profiles during consolidation are shown schematically in Figure 2.

2.2. Testing

2.2.1. DMTA of single tapes

DMTA was performed on single coextruded PP tapes. Specimens were tested in a TA Instruments DMA Q800 DMTA (New Castle, DE, USA) machine operating in a tensile testing mode. The test specimen was cooled to -50°C , allowed to stabilize and then heated at a rate of $3^{\circ}\text{C}\cdot\text{min}^{-1}$ until 150°C . The frequency of oscillation was fixed at 1 Hz and the strain amplitude was $20\ \mu\text{m}$. Storage modulus (E'), loss modulus (E'') and mechanical loss factor ($\tan\delta$) were determined during the test and plotted against temperature.

2.2.2. DMTA of all-PP composites

DMTA of all-PP composite laminates was performed in dual cantilever flexural mode. Specimens were cut from the UD and CP composite plates with dimensions of approximately $60\ \text{mm} \times 15\ \text{mm} \times 2\ \text{mm}$ (length \times width \times thickness) in the same DMTA machine equipped with a data acquisition software. The specimens were cooled to -50°C . The temperature was allowed to stabilize and then the chamber was heated at a rate of $3^{\circ}\text{C}\cdot\text{min}^{-1}$ until 120°C . The specimen was subjected to a sinusoidal flexural displacement applying a maximum tensile strain of 0.1% (which was well within the viscoelastic region) at frequencies 0.01 Hz, 0.1 Hz, 1 Hz, 5 Hz and 10 Hz. For each frequency, the complex dynamic modulus and loss factor were recorded.

2.2.3. Differential scanning calorimetry (DSC)

The crystallinity content of the coextruded tapes and the all-PP composites were characterized from the enthalpy associated during melting using a Mettler-Toledo DSC821 instrument (Greifensee, Switzerland). Heating scans were performed from 25 to 200°C at a heating rate of $10^{\circ}\text{C}/\text{min}$ with nitrogen blanketing inside the sample chamber. An average of three specimens was taken for each measurement. A higher enthalpy of fusion corresponds to the presence of more crystalline domains inside the specimen.

2.2.4. Time-temperature superposition principle

Theoretically and experimentally, dynamic mechanical properties of a polymer (for instance, storage modulus) is influenced by both temperature and frequency (or the response time) of the dynamic loading. This time-dependent behavior implies that the only way to accurately evaluate material performance for a specific application is to test the material under those temperature and time conditions the material will see during application. But there are difficulties in attaining the adequate range of temperatures or frequencies in the laboratory conditions for a specific application. In order to predict the behavior of materials over very high frequencies, the time-temperature superposition (TTS) helps to obtain information about frequencies outside the range that cannot be achieved experimentally. By assuming equivalence of time and temperature, the viscoelastic behavior of a polymer at a chosen reference temperature, T_{ref} , can be related to the viscoelastic behavior of the polymer at a different temperature by a shift, a_T , in the time-scale. For any reference temperature chosen, a fully overlapped curve could be formed, which is called the master curve. It is also widely accepted that a minor vertical shift factor may also be applied to more accurately model master curves [30]. However in this study, a vertical shift factor was not applied.

An attempt was made to apply the TTS to the DMTA data measured as function of both temperature ($T = -50\dots+120^{\circ}\text{C}$) and frequency ($f = 0.01\dots 10\ \text{Hz}$). Master curves in form of storage modulus (E') vs. frequency were produced by superimposing the storage modulus vs. frequency traces using the TTS principle. A reference temperature ($T_{ref} = 22^{\circ}\text{C}$) was used for this superposition (shift-

ing) process. The related shift factor a_T is given by Equation (1):

$$a_T = \frac{E'(T, f)}{E'(T_{ref}, f)} \quad (1)$$

The shift factors of a master curve have some relationship with temperature. Fitting the experimentally determined shift factors to a mathematical model permits the creation of a master curve in form of stiffness vs. frequency. With a multi-frequency measurement, frequencies beyond the measurable range of the DMTA can be achieved by using the superposition method based on the Williams-Landel-Ferry (WLF) equation [31, 32]. For the temperature range above the glass transition temperature, it is generally accepted that the shift factor-temperature relationship is best described by WLF equation (2):

$$\log a_T = \log \left(\frac{f}{f_0} \right) = \frac{-C_1(T - T_{ref})}{C_2 + (T - T_{ref})} \quad (2)$$

where C_1 and C_2 are constants.

For the temperature range below the glass transition temperature, the Arrhenius equation is generally acknowledged as suitable to describe the relationship between the shift factors of the master curve and the temperature. In the latter case, the activation energy (E_a) for shifting the curves can be obtained by Equation (3):

$$\ln a_T = \frac{E_a}{R} \left(\frac{1}{T} - \frac{1}{T_{ref}} \right) \quad (3)$$

3. Results and discussion

3.1. DMTA of PP tape

Figure 3 represents the typical dynamic mechanical behavior of all-PP tapes at 1 Hz frequency. It shows that at temperatures well below 0°C (supposed to be the glassy region of PP) the stiffness is fairly high. With increasing temperature the storage modulus decreases whereas the loss modulus increases, as expected. Above 50°C the stiffness of the tapes drops significantly. Although the tapes lost much of their elastic response above this temperature, their residual stiffness at 120°C (end of the test) is still higher ($E' = 3.2$ GPa) than that of an isotropic PP. The stiffness of the tape at ambient temperature (E' value) is similar to that reported in the literature

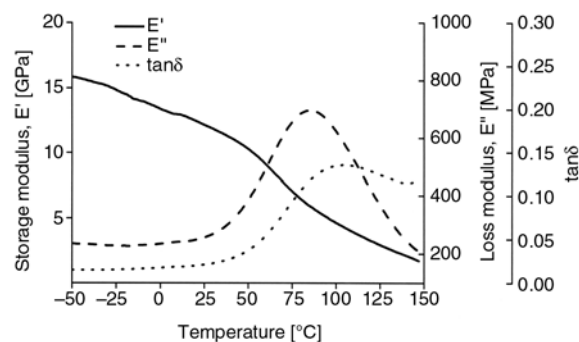


Figure 3. DMA plots of storage modulus, loss modulus and $\tan\delta$ vs. temperature for the PURE® PP tape at frequency 1 Hz

earlier [33, 34]. The high stiffness is attributed to the highly oriented crystals and polymer chains owing to the high draw ratio of the tape. This implies that the tape possesses a residual orientation even at this higher temperature.

Figure 3 also exhibits the correlation of $\tan\delta$ (ratio of E''/E') with temperature, which shows a maximum at $\sim 106^\circ\text{C}$. The maximum $\tan\delta$ value recorded for the all-PP tape was 0.135. Generally, the $\tan\delta$ peaks represent the transition temperatures [32]. However, Figure 3 does not resolve any $\tan\delta$ peak corresponding to the glass-transition of PP ($T_g \sim -10^\circ\text{C} \dots 0^\circ\text{C}$), but a more definite $\tan\delta$ peak is seen corresponding to T_α at approximately 106°C (Figure 2). Since these tapes are produced by high draw ratio (typically > 10), it is reasonable to expect that at such a higher draw ratio, the amorphous phase becomes highly oriented between the crystalline regions and it has less freedom to be involved in segmental motions [35]. Therefore, in highly oriented PP systems, the magnitude of T_g peaks compared to isotropic PP is greatly reduced. The $\tan\delta$ value at around 106°C , corresponding to the α transition (T_α), is believed to be the result of molecular motions which resist the softening effect of the applied heat. While T_g reflects mobility within the amorphous regions, T_α dictates the onset of segmental motion within the crystalline regions [35–37]. A broad peak of α relaxation indicates the delay (retardation) of the relative motion of the lamellae due to the high orientation of the chain segments.

3.2. DMTA of all-PP composites

Figure 4 shows the stiffness of all-PP composites with temperature at a frequency of 1 Hz. At room

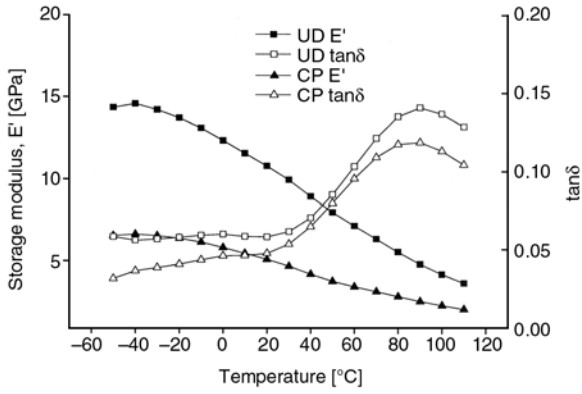


Figure 4. DMA plots of storage modulus and $\tan\delta$ vs. temperature for the all-PP composite laminates with UD and CP lay-ups at frequency 1 Hz

temperature (23°C) the UD and CP all-PP composites possess storage moduli of 10.5 GPa and 5.1 GPa, respectively, which are similar to the previously reported values [29].

The loss factor as a function of temperature for all-PP with UD and CP lay-ups are also shown in Figure 4. Similar to the DMTA data of the single tape, composite specimens also do not show any clear $\tan\delta$ peak corresponding to the β relaxation (T_g). However $\tan\delta$ peak corresponding to the α transition was found to be higher for UD than for CP lay-up.

3.3. Time-temperature superposition (TTS)

Storage modulus for a wider range of frequencies can be obtained by TTS using the data from multi-frequency DMTA tests. Figures 5 and 6 show the variation of storage modulus for a range of temperature between -20°C and 80°C for the all-PP composites having UD and CP lay-ups tested at 0.01 Hz, 0.1 Hz, 1 Hz, 5 Hz and 10 Hz, respec-

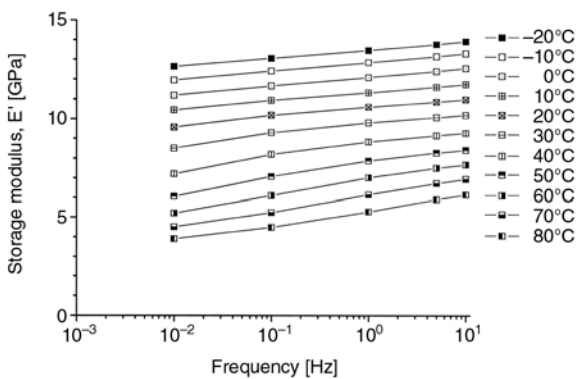


Figure 5. Storage modulus vs. frequency for a range of temperatures for the all-PP composite with UD lay-up

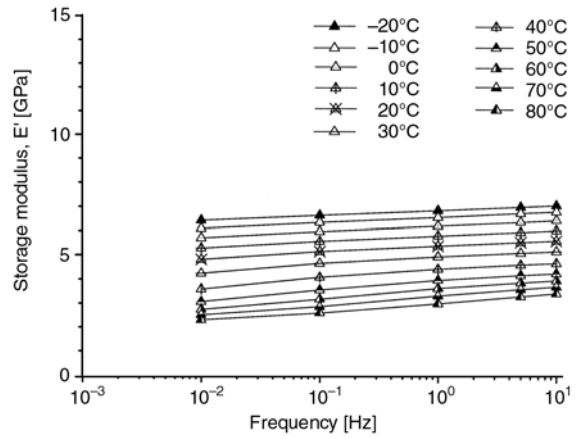


Figure 6. Storage modulus vs. frequency for a range of temperatures for the all-PP composite with CP lay-up

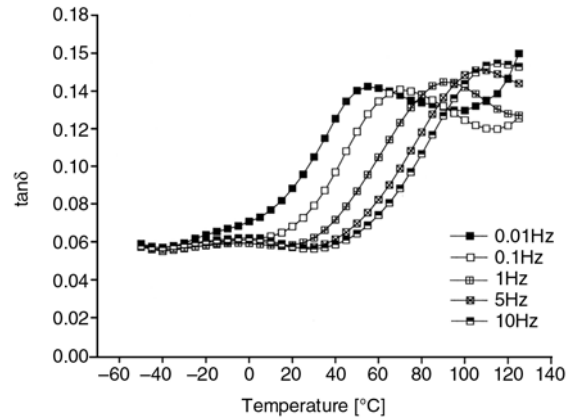


Figure 7. Loss factor ($\tan\delta$) vs. temperature for the all-PP composite with UD lay-up at different frequencies

tively. There is an increase in the storage modulus for both UD and CP with increasing frequency and decreasing temperature, as expected. The variation of $\tan\delta$ with temperature at different frequencies for the UD and CP lay-ups are shown in Figures 7

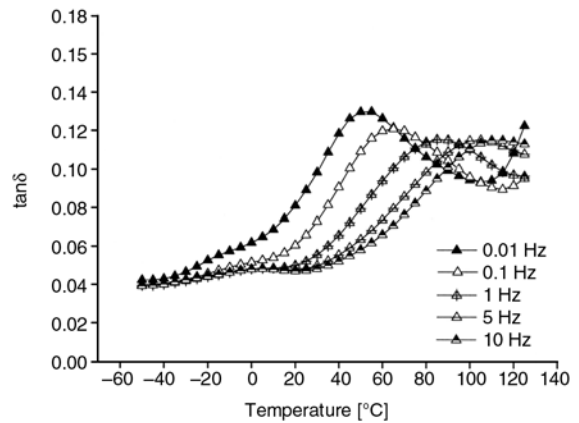


Figure 8. Loss factor ($\tan\delta$) vs. temperature for the all-PP composite with CP lay-up at different frequencies

and 8. A remarkable influence of frequency was observed for the α relaxation of the composites. The frequency increase affected the intensity of $\tan\delta$ and shifted the position of the relaxation region to higher temperatures. The peak became broader and less pronounced due to the additional melting region at higher temperatures. The $\tan\delta$ peak corresponding to the α transition for UD and CP lay-ups were found to be around 89°C and 86°C, respectively, at 1 Hz frequency. The shifting of T_α to higher temperature for UD may arise from higher crystallinity (indicated by higher enthalpy of fusion) of the UD compared to CP composites. The average enthalpies of fusion obtained from the DSC investigations were found to be 105.6 and 102.5 J/g for UD and CP lay-ups, respectively. The shift factors used for the generation of master curves for UD and CP lay-ups are shown in Figure 9. The shift factor plot is slightly curved, reflecting the WLF-type behaviour. The WLF equation was thus selected to relate the shift factors to the temperature. The symbols represent the experimentally determined shift factors, where the lines follow the WLF model. Master curves of the storage modulus and $\tan\delta$ against frequencies created at a reference temperature of 22°C were shown in Figures 10 and 11 respectively, for all-PP composites with UD and CP lay-ups. The storage modulus master curve provides a useful prediction of the modulus over loading frequencies from 10⁻⁹ to 10²⁰ Hz. Similarly the $\tan\delta$ master curves also give an overview to the damping of the material at different frequencies which is useful to measure how well the material can dissipate mechanical energy and very important for the design of material for vibration damping applications. However, it must

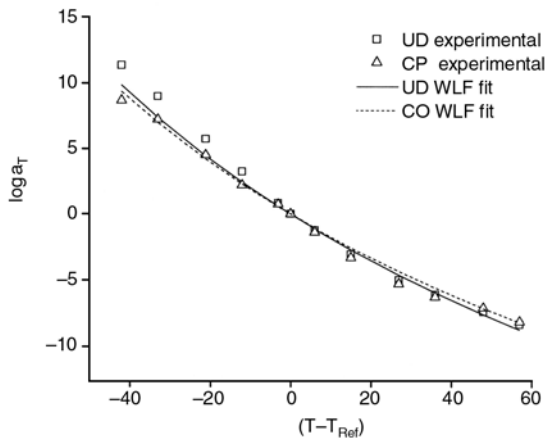


Figure 9. Experimentally determined shift factors and the CP WLF fit

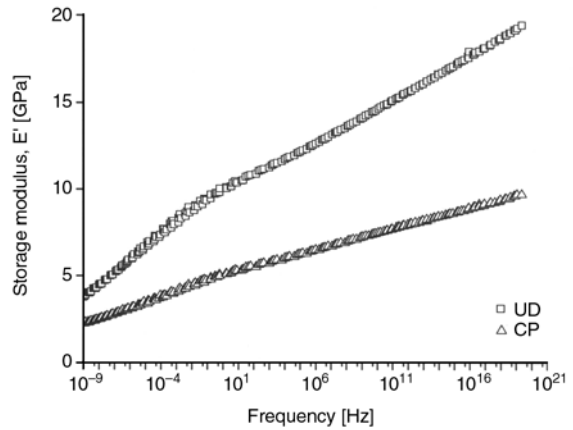


Figure 10. Storage modulus vs. frequency master curves at a reference temperature of 22°C for the all-PP composites with UD and CP lay-ups

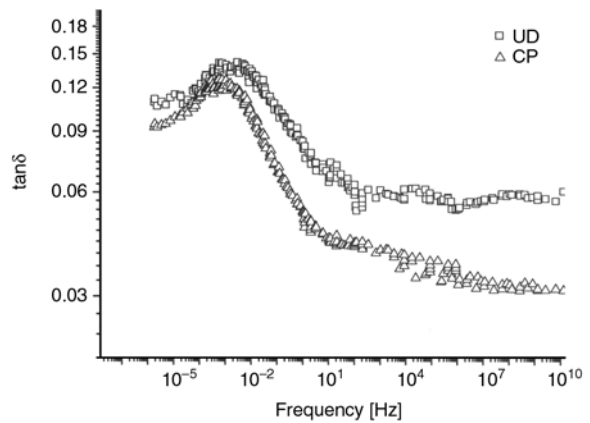


Figure 11. $\tan\delta$ vs. frequency master curves at a reference temperature of 22°C for the all-PP composites with UD and CP lay-ups

be emphasized that these master curves are quite reliable for short term, but significant deviation may occur at large time scales.

The Arrhenius equation was also applied to verify the experimental shift data obtained from the DMTA investigations. In Figure 12, $(\log a_T)$ is thus plotted against the reciprocal of the absolute temperature and the activation energy, E_a , was determined using Equation (4):

$$E_a = m(2.303 \cdot R) \tag{4}$$

where m is the gradient of fit line (in Figure 12) and R is the universal gas constant (8.314 J·K⁻¹·mol⁻¹). The activation energies calculated from the slope of the regression curve were found to be 348 and 307 kJ·mol⁻¹ for UD and CP lay-ups, respectively. Note that they are of the same order as previously reported in the literature [38–41]. The activation energy for shifting the master curve for UD is

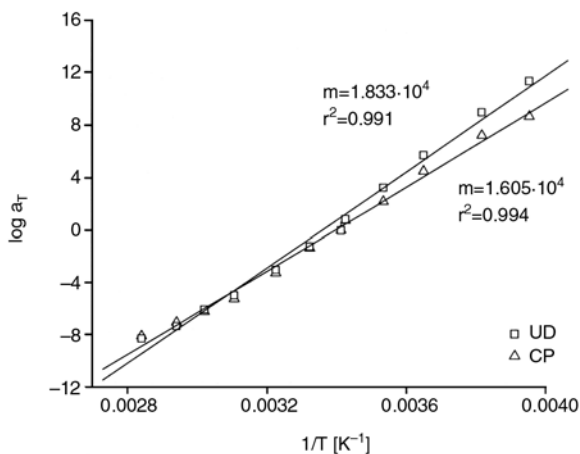


Figure 12. Determination of the activation energy for the all-PP composites with UD and CP lay-ups. Line represents the linear fit

higher than that of CP. Higher activation energy of the all-PP composites with UD lay-up compared to the CP one may be linked with the higher storage modulus of the former.

4. Conclusions

All-PP composites with UD and CP lay-ups were successfully produced from highly oriented coextruded PP tapes (PURE®) by hot consolidation in an autoclave. The dynamic mechanical responses of these tapes and their composites at different frequencies were investigated and analyzed. The storage modulus data obtained from the multi frequency experiments were used to create master curves by assuming time-temperature superposition principle. They can predict the modulus values at frequencies not attainable in the laboratory. The experimental shift factors showed a good agreement with both WLF and Arrhenius models. Using Arrhenius equation, the activation energies required for the UD and CP lay-up composites were calculated. The results showed that higher activation energy was required for shifting the storage modulus curves to obtain the master curve for all-PP composites with UD lay-ups owing to higher stiffness resulting from higher crystallinity (revealed by higher enthalpy of fusion) in the specimens. Additionally, DMTA investigations showed no significant glass transition for the all-PP tapes and their composites due to the high degree of crystallinity and molecular orientation in the all-PP tapes. This is advantageous resulting in a tough failure mode at sub- T_g temperatures and thus broadens the application temperature range of these

recyclable, environment friendly composites toward lower temperatures.

Acknowledgements

The authors thank the German Science Foundation for the financial support of this project (DFG Ka 1202/17)

References

- [1] Capiati N. J., Porter R. S.: The concept of one polymer composites modelled with high density polyethylene. *Journal of Material Science*, **10**, 1671–1677 (1975).
- [2] Loos J., Schimanski T., Hofman J., Peijs T., Lemstra P. J.: Morphological investigations of polypropylene single-fibre reinforced polypropylene model composites. *Polymer*, **42**, 3827–3834 (2001).
- [3] Houshyar S., Shanks R. A.: Morphology, thermal and mechanical properties of poly propylene fibre matrix composites. *Macromolecular Materials and Engineering*, **288**, 599–606 (2003).
- [4] Hine P. J., Ward I. M., Jordan N. D., Olley R. H., Bassett D. C.: The hot compaction behaviour of woven oriented polypropylene fibres and tapes.1. mechanical properties. *Polymer*, **44**, 1117–1131 (2003).
- [5] Ward I. M., Hine P. J.: The science and technology of hot compaction. *Polymer*, **45**, 1413–1427 (2004).
- [6] Hine P. J., Ward I. M., Olley R. H., Bassett D. C.: The hot compaction of high modulus melt-spun polyethylene fibres. *Journal of Material Science*, **28**, 316–324 (1993).
- [7] Yan P. J., Hine P. J., Ward I. M., Olley R. H., Bassett D. C.: The hot compaction of SPECTRA gel-spun polyethylene fibre. *Journal of Material Science*, **32**, 4821–4831 (1997).
- [8] Megremis S. J., Duray S., Gilbert J. L.: Self reinforced composite polyethylene (SRC-PE): a novel material for orthopedic applications. *ASTM Special Technical Publication*, **1346**, 235–255 (1999).
- [9] Hine P. J., Ward I. M., Jordan N. D., Olley R. H., Bassett D. C.: A comparison of the hot-compaction behaviour of oriented, high modulus, polyethylene fibres and tapes. *Journal of Macromolecular Science, Part B: Physics*, **40**, 959–89 (2001).
- [10] Jordan N. D., Olley R. H., Bassett D. C., Hine P. J., Ward I. M.: The development of morphology during hot compaction of tensylon high modulus polyethylene tapes and woven cloths. *Polymer*, **43**, 3397–3404 (2002).
- [11] Rasburn J., Hine P. J., Ward I. M., Olley R. H., Bassett D. C., Kabeel M. A.: The hot compaction of polyethylene terephthalate. *Journal of Material Science*, **30**, 615–622 (1995).
- [12] Hine P. J., Ward I. M.: Hot compaction of woven poly(ethylene terephthalate) multifilaments. *Journal of Applied Polymer Science*, **91**, 2223–2233 (2004).

- [13] Rojanapitayakorn P., Mather P. T., Goldberg A. J., Weiss R. A.: Optically transparent self-reinforced poly(ethylene terephthalate) composites: molecular orientation and mechanical properties. *Polymer*, **46**, 761–773 (2005).
- [14] Hine P. J., Astruc A., Ward I. M.: Hot compaction of polyethylene naphthalate. *Journal of Applied Polymer Science*, **93**, 796–802 (2004).
- [15] Gilbert J. L., Ney D. S., Lautenschlager E. P.: Self-reinforced composite poly(methyl methacrylate)-static and fatigue properties. *Biomaterials*, **16**, 1043–1055 (1995).
- [16] Wright D. D., Lautenschlager E. P., Gilbert J. L.: Bending and fracture toughness of woven self-reinforced composite poly(methyl methacrylate). *Journal of Biomedical Materials Research*, **36**, 441–453 (1997).
- [17] Wright D. D., Gilbert J. L., Lautenschlager E. P.: The effect of processing temperature and time on the structure and fracture characteristics of self-reinforced composite poly(methyl methacrylate). *Journal of Materials Science: Materials in Medicine*, **10**, 503–512 (1999).
- [18] Wright D. D., Lautenschlager E. P., Gilbert J. L.: Hot compaction of poly(methyl methacrylate) composites based on fibre shrinkage results. *Journal of Materials Science: Materials in Medicine*, **16**, 967–975 (2005).
- [19] Hine P. J., Ward I. M.: Hot compaction of woven nylon 6,6 multifilaments. *Journal of Applied Polymer Science*, **101**, 991–997 (2006).
- [20] Pegoretti A., Zanolli A., Migliaresi C.: Flexural and interlaminar mechanical properties of unidirectional liquid crystalline single polymer composites. *Composites Science and Technology*, **66**, 1953–1962 (2006).
- [21] Pegoretti A., Zanolli A., Migliaresi C.: Preparation and tensile mechanical properties of unidirectional liquid crystalline single polymer composites. *Composites Science and Technology* **66**, 1970–1979 (2006).
- [22] Alcock B., Cabrera N. O., Barkoula N. M., Loos J., Peijs T.: The mechanical properties of unidirectional all-polypropylene composites. *Composites, Part A*, **37**, 716–726 (2006).
- [23] Alcock B., Cabrera N. O., Barkoula N. M., Peijs T.: Low velocity impact performance of recyclable all-polypropylene composites. *Composites Science and Technology*, **66**, 1724–1737 (2006).
- [24] Alcock B., Cabrera N. O., Barkoula N. M., Spoelstra A. B., Loos J., Peijs T.: The mechanical properties of woven tape all-polypropylene composites. *Composites, Part A*, **38**, 147–161 (2007).
- [25] Bárány T., Izer A., Czirány T.: On consolidation of self-reinforced polypropylene composites. *Plastics, Rubber and Composites*, **35**, 375–379 (2006).
- [26] Bárány T., Karger-Kocsis J., Czirány T.: Development and characterization of self-reinforced poly(propylene): carded mat reinforcement. *Polymer for Advanced Technologies*, **17**, 818–824 (2006).
- [27] Karger-Kocsis J.: Verbundwerkstoff aus Polypropylenverstärkung und Polypropylenmatrix sowie verschiedene Verfahren zu dessen Herstellung, Patentschrift DE 10237803, Institut für Verbundwerkstoffe GmbH (2007).
- [28] Felix J. M., Gatenholm P.: Formation of entanglements at brushlike interfaces in cellulose-polymer composites. *Journal of Applied Polymer Science*, **50**, 699–708 (1993).
- [29] Alcock B., Cabrera N. O., Barkoula N. M., Reynolds C. T., Govaert L. E., Peijs T.: The effect of temperature and strain rate on the mechanical properties of highly oriented polypropylene tapes and all-polypropylene composites. *Composites Science and Technology*, **67**, 2061–2070 (2007).
- [30] Ward I. M., Sweeney J.: An introduction to the mechanical properties of solid polymers. Wiley, New York (2004).
- [31] Williams M. L., Landel R. F., Ferry J. D.: The temperature dependence of relaxation mechanisms in amorphous polymers and other glass forming liquids. *Journal of American Chemical Society*, **77**, 3701–3707 (1955).
- [32] Ferry J. D.: Viscoelastic properties of polymers, Wiley, New York (1970).
- [33] Yang J., Chaffey C. E., Vancso G. J.: Structure, transitions, and mechanical properties of polypropylene oriented by roll-drawing. *Plastic Rubber and Composites Processing and Applications*, **21**, 201–210 (1994).
- [34] Tariya A. K., Richardson A., Ward I. M.: Production and properties of highly oriented polypropylene by die drawing. *Journal of Applied Polymer Science*, **33**, 2559–2579 (1987).
- [35] Boyd R. H.: Relaxation processes in crystalline polymers: molecular interpretation- a review. *Polymer*, **26**, 1123–1133 (1985).
- [36] Hu W. G., Schmidt-Rohr K.: Polymer ultradrawability: the crucial role of alpha relaxation chain mobility in the crystallites. *Acta Polymerica*, **50**, 271–285 (1999).
- [37] Roy S. K., Kyu T., St. John Manley R.: Mechanical relaxations of oriented gelation-crystallized polyethylene films. *Macromolecules*, **21**, 1741–1756 (1988).
- [38] Ariyama T., Mori Y., Kaneko K.: Tensile properties and stress relaxation of polypropylene at elevated temperatures. *Polymer Engineering and Science*, **37**, 81–90 (1997).
- [39] Faucher J. A.: Viscoelastic behaviour of polyethylene and polypropylene. *Journal of Rheology*, **3**, 81–93 (1959).
- [40] Klompen E. T. J., Govaert L. E.: Nonlinear viscoelastic behaviour of thermorheologically complex materials. *Mechanics of Time-Dependent Materials*, **3**, 46–69 (1999).
- [41] Amash A., Zugenmaier P.: Thermal and dynamic mechanical investigations on fiber-reinforced polypropylene composites. *Journal of Applied Polymer Science* **63**, 1143–1154 (1996).